Research Article
Vol. 60, No. 13 / 1 May 2021 / Applied Optics 3677

applied optics

Optical wireless communication performance enhancement using Hamming coding and an efficient adaptive equalizer with a deep-learning-based quality assessment

Bidaa Mortada,[1] Hanan S. Ghanem,[2] Randa S. Hammad,[1] Safie El-Din Nasr Mohamed,[2,*] Ahmed Sedik,[3] Rania A. Eltaieb,[1] Walid El-Shafai,[1,10] Ahmed Nabih Zaki Rashed,[1] Mohsen A. M. El-Bendary,[4] Mohammed Salah F. Tabbour,[1] Ghada M. El Banby,[5] Ashraf A.M. Khalaf,[2] Ahmed E. A. Farghal,[6] HossamEl-din H. Ahmed,[1] Gamal A. Hussein,[7] El-Sayed M. El-Rabaie,[1] Ibrahim M. Eldokany,[1] Moawad I. Dessouky,[1] Abdelnaser A. Mohamad,[1] O. Zahran,[1] Maha Elsabrouty,[8] Hesham F. A. Hamed,[2] Gerges M. Salama,[2] Said E. El-Khamy,[9] Hossam M. H. Shalaby,[8,9] and Fathi E. Abd El-Samie[1,11]

[1]Department of Electronics and Electrical Communications Engineering, Faculty of Electronic Engineering, Menoufia University, Menouf 32952, Egypt
[2]Department of Electrical Engineering, Faculty of Engineering, Minia University, Minia 61111, Egypt
[3]Department of the Robotics and Intelligent Machines, Faculty of Artificial Intelligence, Kafr El Sheikh University, Kafr El Sheikh, Egypt
[4]Department of Electronics Technology, Faculty of Technology and Education, Helwan University, Cairo, Egypt
[5]Department of Industrial Electronics and Control Engineering, Faculty of Electronic Engineering, Menoufia University, Menouf 32952, Egypt
[6]Electrical Engineering Department, Faculty of Engineering, Sohag University, 82524 Sohag, Egypt
[7]Engineering Sector of Broadcast Egyptian Radio and Television Union Cornish El Nile, P.O. Box 1186, Cairo, Egypt
[8]Department of Electronics and Communication, Egypt-Japan University of Science and Technology, Alexandria, Egypt
[9]Electrical Engineering Department, Faculty of Engineering, Alexandria University, Alexandria, Egypt
[10]Security Engineering Lab, Computer Science Department, Prince Sultan University, Riyadh 11586, Saudi Arabia
[11]Department of Information Technology, College of Computer and Information Sciences, Princess Nourah Bint Abdulrahman University, Riyadh 21974, Saudi Arabia

*Corresponding author: sofianmohamed84@gmail.com

Received 11 January 2021; revised 1 March 2021; accepted 2 March 2021; posted 3 March 2021 (Doc. ID 418438); published 23 April 2021

Optical wireless communication (OWC) technology is one of several alternative technologies for addressing the radio frequency limitations for applications in both indoor and outdoor architectures. Indoor optical wireless systems suffer from noise and intersymbol interference (ISI). These degradations are produced by the wireless channel multipath effect, which causes data rate limitation and hence overall system performance degradation. On the other hand, outdoor OWC suffers from several physical impairments that affect transmission quality. Channel coding can play a vital role in the performance enhancement of OWC systems to ensure that data transmission is robust against channel impairments. In this paper, an efficient framework for OWC in developing African countries is introduced. It is suitable for OWC in both indoor and outdoor environments. The outdoor scenario will be suitable to wild areas in Africa. A detailed study of the system stages is presented to guarantee the suitable modulation, coding, equalization, and quality assessment scenarios for the OWC process, especially for tasks such as image and video communication. Hamming and low-density parity check coding techniques are utilized with an asymmetrically clipped DC-offset optical orthogonal frequency-division multiplexing (ADO-OFDM) scenario. The performance versus the complexity of both utilized techniques for channel coding is studied, and both coding techniques are compared at different coding rates. Another task studied in this paper is how to perform efficient adaptive channel estimation and hence equalization on the OWC systems to combat the effect of ISI. The proposed schemes for this task are based on the adaptive recursive least-squares (RLS) and the adaptive least mean squares

1559-128X/21/133677-12 Journal

(LMS) algorithms with activity detection guidance and tap decoupling techniques at the receiver side. These adaptive channel estimators are compared with the adaptive estimators based on the standard LMS and RLS algorithms. Moreover, this paper presents a new scenario for quality assessment of optical communication systems based on the regular transmission of images over the system and quality evaluation of these images at the receiver based on a trained convolutional neural network. The proposed OWC framework is very useful for developing countries in Africa due to its simplicity of implementation with high performance.

https://doi.org/10.1364/AO.418438

1. INTRODUCTION

Radio frequency (RF) communication is the most widely used type of wireless communication systems. A drawback of the RF technology is that it is not able to fulfill the requirements of users as the demand for bandwidth is increasing significantly with the increase of the number of users [1]. In addition, RF communication systems suffer from high installation costs, bandwidth limitations, low data rates, and security issues. Optical wireless communication (OWC) technology is one of the alternatives for addressing the RF limitations. It offers high data rates, unlimited license-free bandwidth, low installation cost, and high security [2].

Visible light communication (VLC) is the indoor version of the OWC. The VLC suffers from the multipath effect, which leads to multiple copies of the data at the receiver and hence leads to intersymbol interference (ISI) [3]. It is known that communication over noisy channels cannot guarantee error-free reception of data. Hence, forward-error-correction (FEC) codes are utilized to encode user data in blocks called codewords for robust transmission over noisy communication links [4]. The point-to-point and diffused configurations are the two most common VLC system configurations. The point-to-point system is considered the simplest one, where both the transmitter and receiver point to each other with a line-of-sight (LOS) path. The diffuse VLC is very flexible and does not require an exact alignment of the transmitter and receiver modules [5]. However, for a horizontal separation of 5 m, diffuse links experience generally a 50–70 dB path loss. A second drawback is that the received signal can also suffer from severe multipath dispersion and an unequalized bit rate with a room volume of $10 \times 10 \times 3\ \mathrm{m}^3$. Moreover, dispersion-induced ISI can lead to a power penalty, and hence bit-error-rate (BER) degradation. All these factors necessitate the need to increase the amount of transmitted optical power [6]. The most commonly used modulation scheme for practical VLC systems is intensity modulation/direct detection (IM/DD) [7].

The free-space optical (FSO) technology is the only solution when the optical fiber connection is not a practical solution, and where a high bandwidth is requested. The best wireless technology, which can have a huge bandwidth of several gigabits per second, is the FSO [8,9]. For the implementation of FSO communication systems between buildings or in wild areas for multimedia applications, arrays of laser links can be used. The channel in this case is the free space including the Earth's atmosphere. Hence, this channel is subject to several impairments for light wave communication including heavy rain in wild areas, dust particles in dessert areas, and fog in agriculture areas. All these scenarios are widely encountered in Africa. Hence, the received light waves suffer different types of distortion including noise and ISI due to pulse spreading. That is why equalization and error correction coding are badly needed in FSO systems [10].

Hussien *et al*. [11] studied the performance of OWC systems from the equalization perspective. They investigated adaptive channel estimation algorithms with activity detection guidance (ADG). This work lacks the study of a unified framework for FSO systems with channel estimation and equalization incorporated as a step in the system. The adaptive channel estimation must ensure convergence of the algorithm. Convergence of adaptive algorithms has generally been studied in the literature with certain constraints on the adaptive algorithm step size based on the eigen-distribution of correlation matrices. There is a need to achieve a trade-off between the requirement to achieve the convergence and the speed of convergence. This issue is studied in detail in [12].

Orthogonal frequency-division multiplexing (OFDM) is currently the leading multicarrier modulation technology. It is used to transmit the data stream over several subcarriers, orthogonally [13]. Unfortunately, conventional OFDM is not suitable for IM/DD optical communication because of its bipolar symbol shape [14]. A unipolar OFDM can be implemented through several techniques such as asymmetrically clipped direct-current offset optical OFDM (ADO-OFDM) [15]. In the proposed framework, we will adopt ADO-OFDM for the VLC scenario.

In 1962, Gallager proposed the low-density parity-check (LDPC) code [16]. However, it was neglected for many years because it was impractical to implement. After that, MacKay and Neal rediscovered it again in their work [17]. We will adopt LDPC coding in the proposed VLC framework and also compare it with Hamming coding. In addition, we will present efficient adaptive channel estimation schemes to overcome the effect of ISI due to multipath dispersion and atmospheric impairments in all OWC systems. Moreover, a convolutional neural network (CNN)-based algorithm is presented for quality assessment of optical communication systems based on regular transmission of certain image patterns on the optical link.

The rest of the paper is organized as follows. The proposed framework for optical communication is presented in Section 2. The VLC model, FSO model, error correction coding, and adaptive channel estimation are presented in Section 3. The proposed quality assessment algorithm based on CNNs is presented in Section 4. The simulation results are given in Section 5. Finally, Section 6 introduces the concluding remarks.

2. PROPOSED COMMUNICATION FRAMEWORK

This paper presents a unified framework for OWC systems, especially for multimedia applications. The block diagram of

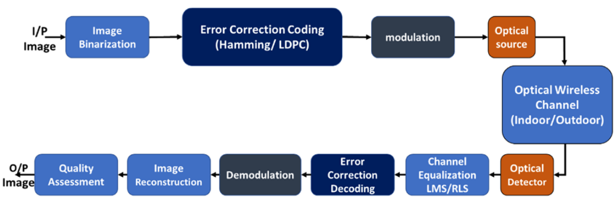

Fig. 1. Proposed WOC framework.

the proposed optical communication framework is included in Fig. 1.

The input image is first converted to binary digits, and then error correction coding is implemented with either a Hamming or LDPC code, and finally modulation is performed at the transmitter. This framework can be implemented in both VLC and FSO scenarios. At the receiver side, channel estimation is performed with either a least mean squares (LMS) or recursive least-squares (RLS) algorithm with ADG and tap decoupling (TD) in order to perform the equalization process. Error correction decoding and demodulation are then performed. Finally, quality assessment of the obtained images is performed with a pretrained CNN.

The main contributions of this paper can be summarized as follows:

I. Introduction of a general framework for OWC communication for multimedia applications in African countries with different terrains.
II. Utilization of efficient coding schemes (Hamming and LDPC) in the proposed OWC framework and comparison between them.
III. Investigation of the ADO-OFDM modulation technique in the proposed framework.
IV. Development of efficient adaptive signal processing techniques to deal with the channel estimation problem for efficient equalization in OWC systems.
V. Development of an image quality assessment algorithm based on CNNs to rate the OWC channel quality.

The different tasks to be implemented in the proposed framework will be presented in detail in Section 3.

3. SYSTEM MODELS, CODING, AND CHANNEL ESTIMATION

A. VLC and FSO System Models

The VLC model uses the light band from the electromagnetic spectrum, which expands from 380 to 780 nm. VLC introduces a new standard known as light fidelity (Li-Fi), which is the optical equivalent to wireless fidelity (Wi-Fi). The VLC system model in [18] is considered in our work. The channel in the FSO communication scenario includes the Earth's atmosphere, and several degradations are encountered due to rain, dust, and fog in addition to the multipath effect. Non-negative real signals can be generated using several OFDM techniques for IM/DD optical systems. ADO-OFDM is one of these techniques, and it is said to be a merged structure of ACO-OFDM and DCO-OFDM [19]. However, it is more efficient than both of them from the optical power perspective [19]. Figure 2 shows a general block diagram of the ADO-OFDM technique that will be adopted in the proposed framework. The detailed mathematical model of the ADO-OFDM can be found in [20–22].

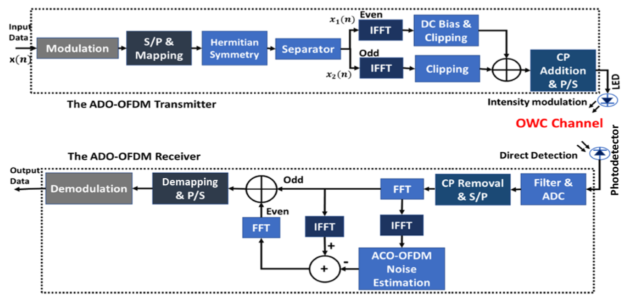

Fig. 2. General block diagram for the ADO-OFDM technique [18].

B. Error Correction Coding

The emergence of large-scale, high-speed data networks has increased the demand for efficient and reliable digital communication systems [23]. Channel coding is used to save the signal from the channel effects of interference and noise. It improves communication performance by adding redundancy to the message before being transmitted [24]. Channel codes are widely used in modern digital communication systems to provide reliable data transfer as in mobile, satellite, radio, video, and optical communications.

1. *LDPC Coding*

The LDPC is a class of linear block codes that is characterized by a sparse parity-check matrix **H**, which contains a few 1s [22]. The LDPC code can be represented via matrices or by using the graphical representation as introduced by Tanner [16]. The parity-check matrix is often randomly generated with dimensions ($m \times n$), where m represents the number of rows and n represents the number of columns.

The LDPC coding is recommended for higher code rates such as (3/4) and (7/8), because it has less decoding complexity and better coding performance compared with that of the Turbo code [25].

2. *Hamming Coding*

Hamming coding was introduced as the first leap toward the error-correcting codes by R. W. Hamming in 1950. The Hamming (7, 4) code is considered the default Hamming code. It represents an original message of 4-bits encoded with 7-bit codewords. This code can detect two errors, and only one error can be corrected [26]. For single error correction, the Hamming code should have a number of parity bits not less than 3 [26]. For double detection and single correction, Hamming codes proved to be one of the most efficient parity-check codes, since they maximize the distance between codewords.

C. Channel Estimation

Figure 3 shows the OWC system depending on an LMS channel estimation algorithm with ADG and TD. The transmitter converts an electrical input signal into an optical output by a laser diode or a LED. This optical data X_j with data rate R_b is

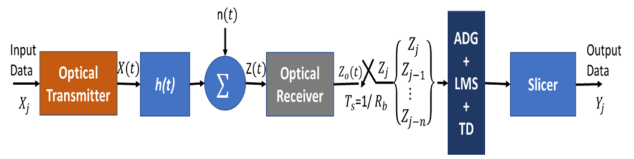

Fig. 3. OWC system implementing LMS channel estimation algorithm based on ADG with TD.

transmitted, and it experiences dispersion through a multipath dispersive channel. The $n(t)$ is the additive white Gaussian noise (AWGN). It corrupts the transmitted optical signal. At the receiver side, the photodetector converts the received optical signal $Z(t)$ to an electrical signal.

The ISI problem in OWC systems leads to some pulse spreading, and hence some sort of tap coupling occurs. To facilitate the equalization process, there is a need to perform TD. The channel estimation process using the ADG with the TD concept has been studied in the literature in [27] to mitigate the ISI problem. In this paper, the same concept of adaptive channel estimation with ADG and TD is adopted in OWC systems. Activity detection is performed to determine the inactive taps that are decoupled and disregarded in the adaptive channel estimation process, which speeds up the convergence behavior of the LMS algorithm [28]. The activity measure with the LMS algorithm is given as follows:

$$A(i) = \frac{\sum_{n=1}^{N}\left[\left\{d(i) - y(i) + w(i)x(n-i+1)\right\}\cdot x(n-i+1)\right]^2}{\sum_{n=1}^{N}\left[x(n-i+1)\right]^2}, \quad (1)$$

where d is the desired signal, x is the input signal, i is the tap index, n is the time index, $w(i)$ is the estimated channel impulse response at tap i, and N is the number of input samples. The activity $A(i)$ must exceed a certain threshold to accept the tap as follows:

$$A(i) > \sum_{n=1}^{N}\frac{[d(n)]^2.\log(n)}{n}. \quad (2)$$

Another alternative for channel estimation is the RLS algorithm. For this algorithm, the activity measure is given as [29]

$$A(i) = \frac{\sum_{n=1}^{N}[d(i)\cdot x(n-i+1)]^2}{\sum_{n=1}^{N}[x(n-i+1)]^2}. \quad (3)$$

A thresholding process is also implemented in this scenario according to [30]:

$$A(i) > \sum_{n=1}^{N}\frac{[d(n)]^2.\log(n)}{n}. \quad (4)$$

To remove the effect of tap coupling in colored input scenarios, the activity function is modified as follows [31]:

$$A'(i) = \frac{\sum_{n=1}^{N}\left[\left\{d(i) - y(i) + w(i)x(n-i+1)\right\}\cdot x(n-i+1)\right]^2}{\sum_{n=1}^{N}\left[x(n-i+1)\right]^2}. \quad (5)$$

This modification enhances the channel estimation in the case of colored inputs [32].

4. IMAGE QUALITY ASSESSMENT

The proposed model for quality level assessment of the communication process estimates the degradation level due to the optical communication channel. It is based on the transmission of zebra chart patterns over the optical communication channel, regularly. The level of quality of the received patterns reflects the quality of the communication process. Both visible and IR images have been used for this objective. Some images have been collected for both scenarios of high and low quality. A pretrained CNN is used to determine the quality level of the received patterns. The operation of the CNN depends on a convolutional layer for feature extraction, pooling, and drop-out layers for feature reduction, and finally a fully connected layer for classification of quality level [33–35].

Different convolution masks with different sizes and orientations are implemented in the convolutional layer. The objective of this layer is to generate feature maps of the images to be assessed. A pooling layer with max-pooling strategy is adopted in the proposed quality assessment algorithm to reduce dimensionality of feature maps. A rectified linear unit (ReLU) is adopted to induce a clipping effect for negative values. A softmax algorithm is adopted in the fully connected layer to yield the classification result for the received image. A CNN structure comprising six convolutional layers with 16, 32, 64, 128, 256, and 512 filters for layers 1, 2, 3, 4, 5 and 6, respectively, in addition to six max-pooling layers, is adopted in the proposed quality assessment algorithm. The image size used for regular transmission of patterns is 224 × 224.

5. SIMULATION RESULTS AND DISCUSSION

In this section, computer simulation experiments are presented to check the efficiency of the proposed OWC framework. The employed simulation parameters for the proposed coded ADO-OFDM technique for the VLC model are introduced in [18].

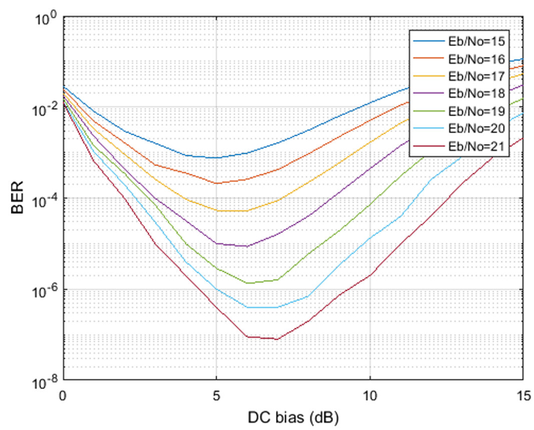

Fig. 4. BER versus DC bias (dB) with different values of $\frac{E_b}{N_o}$(dB) showing the optimal DC bias value and the corresponding BER.

A. Hamming versus LDPC Coding in VLC Model

The DC bias value is affected by the signal modulation constellation size and the value of the peak-to-average power ratio (PAPR) of the OFDM signal.

In Fig. 4, the BER performance is plotted versus the DC bias for different values of E_b/N_o. It can be noticed that the curves have minimum values at which the optimum DC bias is obtained; i.e., for $E_b/N_o = 15$ dB, the optimum value of the DC bias is around 4 dB.

The simulation results are discussed in this section for the performance evaluation of both coding techniques considering the size of the IFFT/FFT frame as $N = 4096$, and the cyclic prefix length as 24. The BER versus the signal-to-noise ratio (E_b/N_o) is studied for both coding techniques with different coding rates, as mentioned in Table 1, at different levels of DC bias (3 and 7 dB) assuming an AWGN channel model.

The simulated BER output in Figs. 5(a) and 5(b) is estimated for a coded ADO-OFDM system with Hamming codes $(7, 4)$, $(15, 11)$, $(31, 26)$, and $(63, 57)$ and an uncoded ADO-OFDM system for 3 dB and 7 dB SNR, respectively.

Table 1. Coding Rates for Hamming and LDPC Codes

Coding Rate	Hamming Code	LDPC Code
1/2	$(7,\ 4) = 0.57$	$(4000,\ 2000) = 0.50$
3/4	$(15,\ 11) = 0.73$	$(4000,\ 3000) = 0.75$
4/5	$(31,\ 26) = 0.83$	$(4000,\ 3200) = 0.80$
9/10	$(63,\ 57) = 0.90$	$(4000,\ 3600) = 0.90$

By increasing the length of the Hamming code, the number of redundant bits will increase and the simulated BER performance is degraded.

Figures 6(a) and 6(b) show the simulated BER for the LDPC-coded ADO-OFDM system with coding rates $(1, 2)$, $(3, 4)$, $(4, 5)$, and $(9, 10)$ and the uncoded ADO-OFDM system for 3 dB and 7 dB SNR, respectively. The simulated output shows that for a fixed error correction capability, as the code length of the LDPC code is increased, the performance deteriorates. This increase in code rate means a reduction in the number of redundant bits, which is responsible for performance degradation.

Figure 7 shows the simulated BER performance comparison between Hamming coding and LDPC coding with different coding rates at a DC bias of 3 dB. The simulation results indicate that the simulated BER performance of the LDPC coded system outperforms that of the Hamming coded system as shown in Fig. 7(a). However at low E_b/N_o values, the Hamming code is better than the LDPC code up to 12 dB as shown in Figs. 7(b) and 7(c). By increasing the E_b/N_o values larger than 15 dB, the LDPC code dominates in performance as shown in Fig. 7(d).

Moreover, Fig. 8 shows the simulated BER performance comparison between Hamming coding and LDPC coding with different coding rates at a DC bias of 7 dB. The simulated output shows that the Hamming BER performance is better at low E_b/N_o values up to 12 dB than that of the LDPC

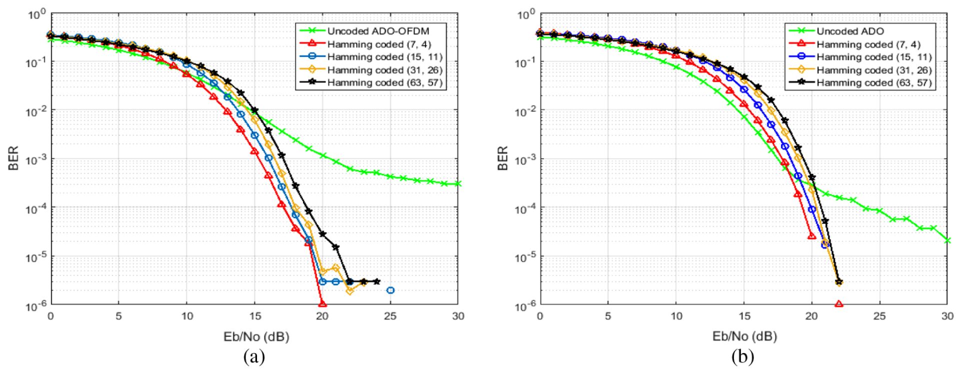

Fig. 5. BER performance for the uncoded ADO-OFDM system and the Hamming coded system with different coding rates at DC bias: (a) 3 dB and (b) 7 dB.

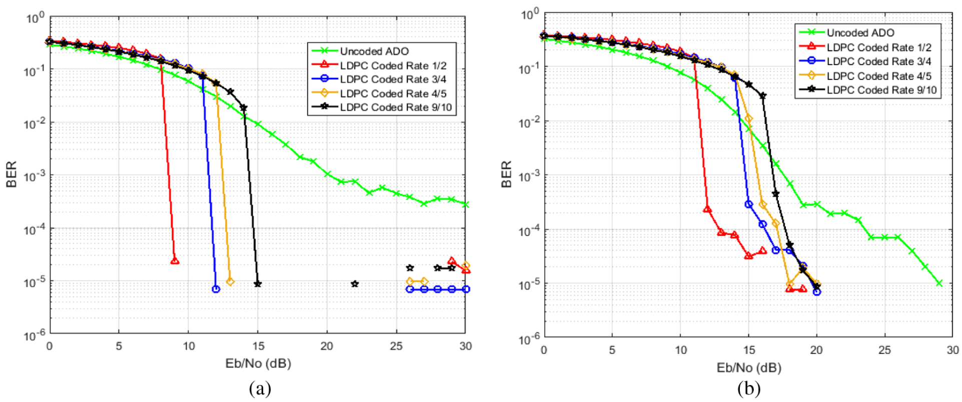

Fig. 6. BER performance for the uncoded ADO-OFDM system and the LDPC coded system with different coding rates at DC bias: (a) 3 dB and (b) 7 dB.

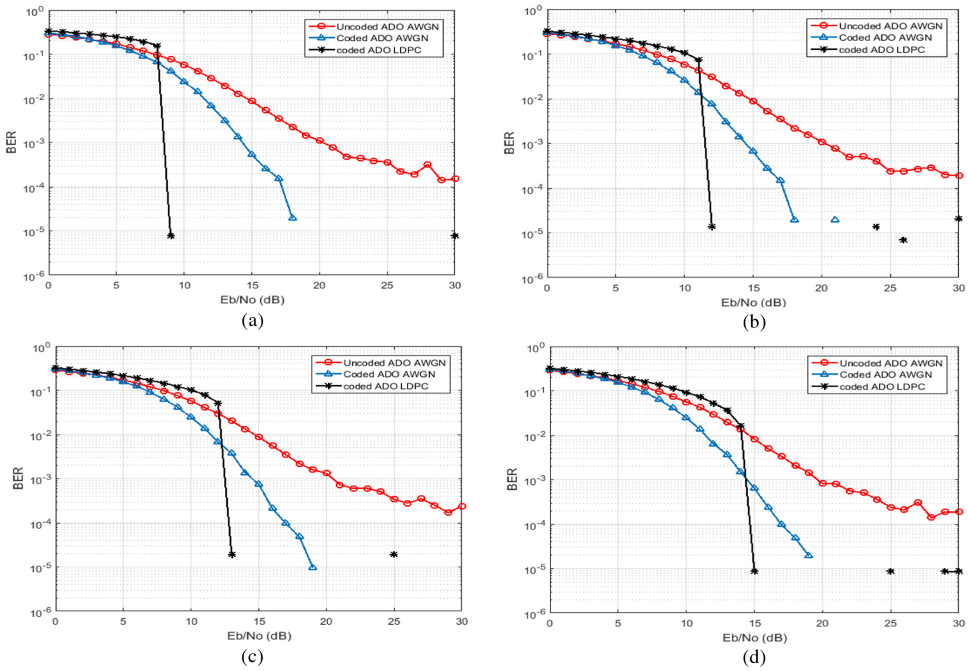

Fig. 7. BER performance comparison between Hamming coding and LDPC coding at a DC bias of 3 dB with different coding rates: (a) 1/2, (b) 3/4, (c) 4/5, and (d) 8/9.

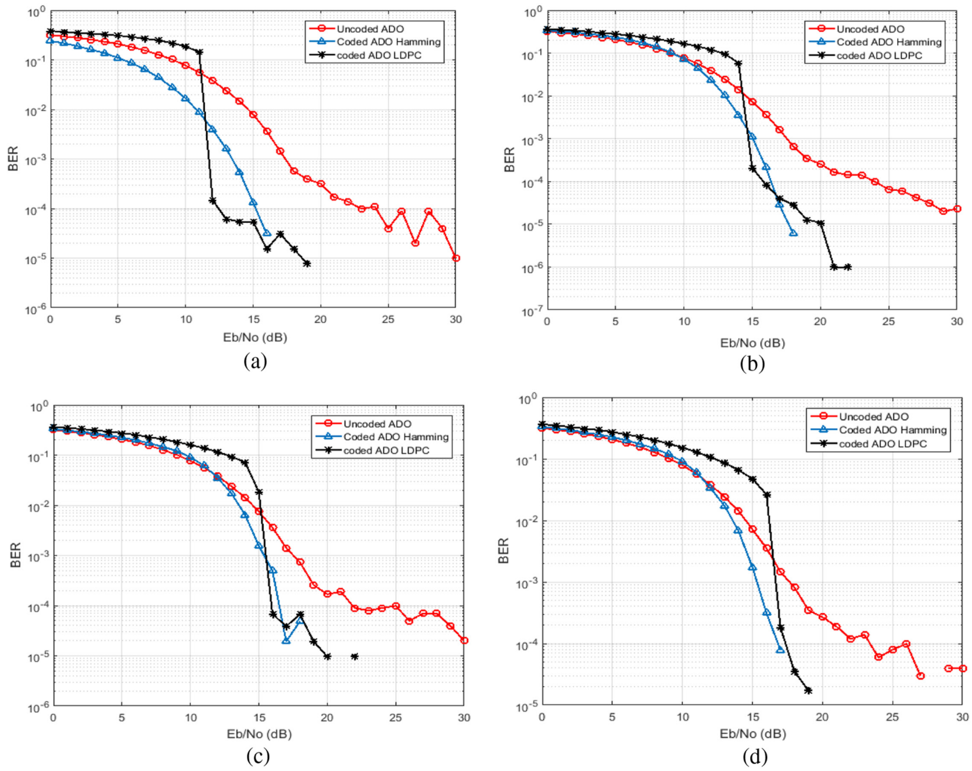

Fig. 8. BER performance comparison between Hamming coding and LDPC coding at a DC bias of 7 dB with different coding rates: (a) 1/2, (b) 3/4, (c) 4/5, and (d) 8/9.

code. Also, the simulation results indicate degradation in the LDPC code BER performance with the increase in the coding rate.

Table 2 shows the BER performance comparison between Hamming coding and LDPC coding for ADO-OFDM at $\mathrm{BER} = 10^{-3}$. Figure 9 shows the simulation times for the decoding processes of LDPC and Hamming codes for handling the same amount of data. These times indicate that for handling the same amount of data, Hamming coding requires much less time compared to LDPC coding.

Table 2. BER Performance Comparison Between Hamming and LDPC Codes for ADO-OFDM at BER = 10^{-3}

DC Bias	3 dB				7 dB			
Coding rate (R)	1/2	3/4	4/5	8/9	1/2	3/4	4/5	8/9
Hamming code	13	14	15	13	13	15	15.5	15.5
LDPC code	8.5	11.5	12.5	14	12	15	15.5	16.5

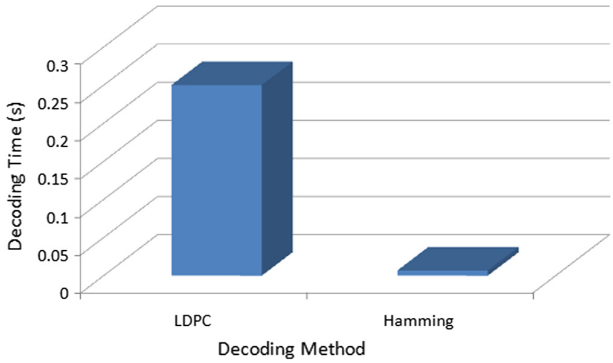

Fig. 9. Complexity evaluation with decoding time for Hamming and LDPC coding.

B. Adaptive LMS Channel Estimation Experiments

The standard adaptive LMS algorithm cannot distinguish between active and inactive taps, and hence it cannot mitigate the ISI problem. Figure 10 shows the convergence behavior of the squared error versus the number of iterations. It is clear that the LMS algorithm with ADG and TD has a fast convergence. Figure 11 indicates the number of estimated channel active taps versus the number of iterations. We can notice that the proposed algorithm can detect three active taps at the iteration number 3751 and eliminate the inactive ones from the channel tap estimation, and hence it can mitigate the problem of ISI.

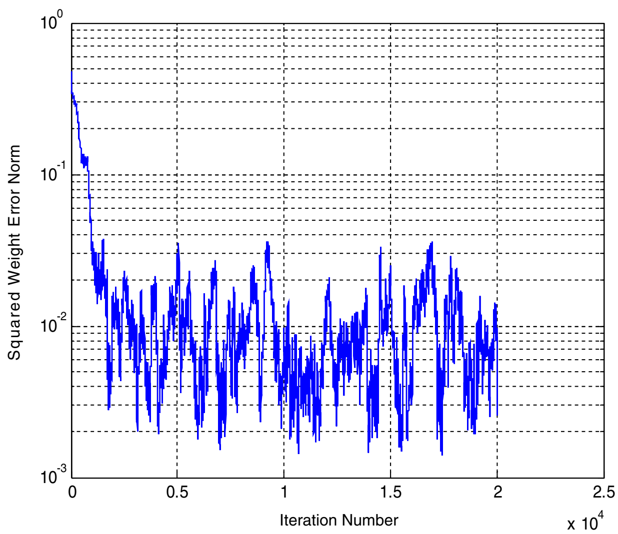

Fig. 10. Squared weight-error norm performance using LMS algorithm with ADG and TD.

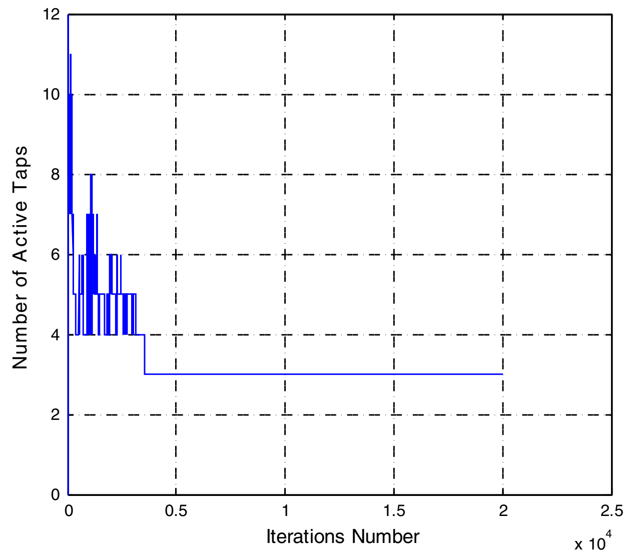

Fig. 11. Estimated active channel taps.

C. RLS Adaptive Channel Estimation Results

The MATLAB package is utilized to simulate the proposed scenario using an adaptive RLS channel estimation algorithm with ADG and TD. Table 3 shows the input parameters used in this simulation experiment. Figure 12 shows the supposed impulse response of the unknown multi-tap channel, which will be estimated. The RLS algorithm is used with an initial input covariance estimate of 0.009 and a forgetting factor of 0.99.

Table 3. Input Simulation Parameters for the Scenario of the RLS Algorithm

Input Parameters	Values
Input signal	Random signal
Number of iterations	5040
Number of channel taps	40
Adaptive filter order	40
AWGN variance	0.1
Forgetting factor	0.99

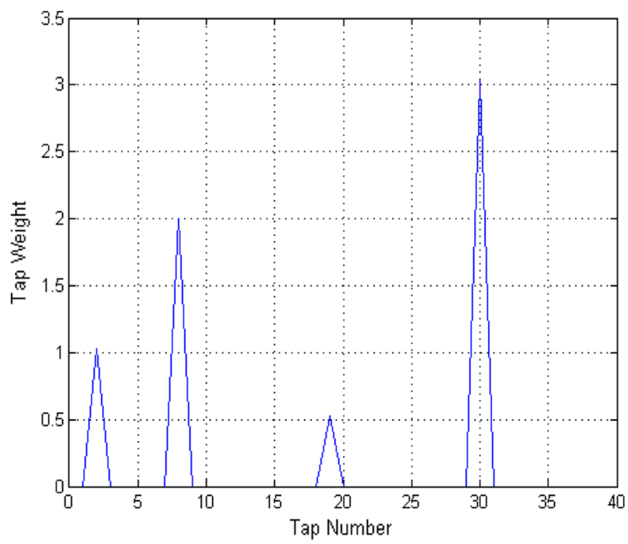

Fig. 12. Supposed impulse response of the multi-tap channel.

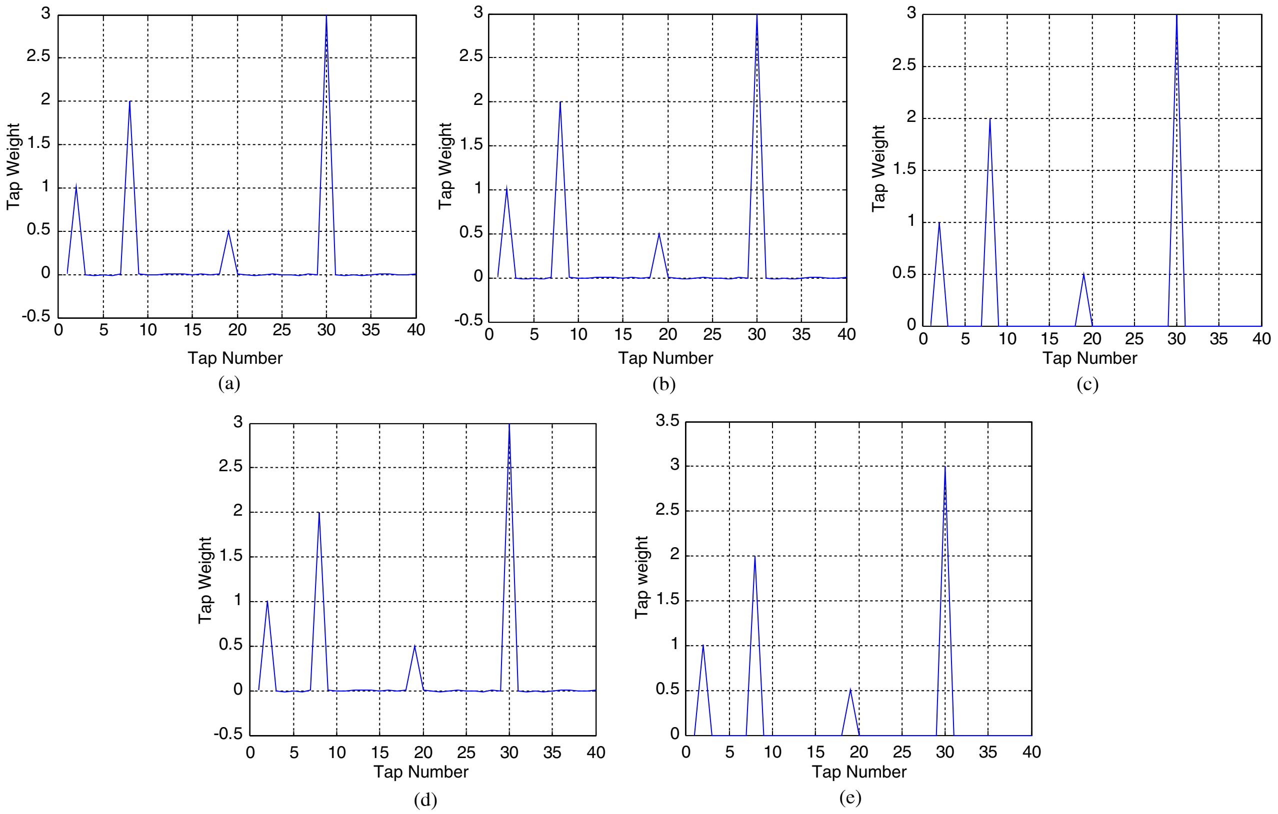

Fig. 13. (a) Estimated channel impulse response by the standard RLS algorithm for white input. (b) Estimated channel impulse response by the standard RLS algorithm for colored input. (c) Estimated channel impulse response by the RLS algorithm with ADG for white input. (d) Estimated channel impulse response by RLS algorithm with ADG for colored input. (e) Estimated channel impulse response by the RLS algorithm with TD for colored input.

Figure 13 shows the RLS channel estimation results. It is clear from the parts of this figure that the RLS algorithm with ADG and TD manages to estimate the channel impulse response correctly, even with colored inputs.

Figure 14 shows the asymptotic behavior of the standard RLS algorithm and the RLS algorithm with ADG for white inputs. It is clear that the RLS algorithm with ADG has a fast convergence. It can converge after about 1000 iterations. Figure 15 shows the asymptotic behavior for the standard RLS algorithm, RLS algorithm with ADG, and RLS algorithm with ADG and TD for colored inputs.

We can deduce that both the standard RLS algorithm and the RLS algorithm with ADG have the same bad asymptotic behavior. However, the RLS algorithm with ADG and TD has the best asymptotic behavior, and it has the fastest convergence after about 1700 iterations. Figure 16 shows the number of active taps, which can be estimated using the standard RLS algorithm and the RLS algorithm with ADG in the case of a white input signal. We notice that the RLS algorithm with ADG can estimate the correct channel taps, while the standard RLS cannot estimate the original channel taps, because the standard RLS algorithm for white inputs deals with all taps as being active, and hence it gives values for those non-active taps. Figure 17 shows the number of active taps that can be estimated by the standard RLS algorithm, the RLS algorithm with ADG, and the RLS algorithm with ADG and TD in the case of colored inputs. We can find that the true number of the original channel taps can be estimated only by the RLS algorithm with ADG and TD.

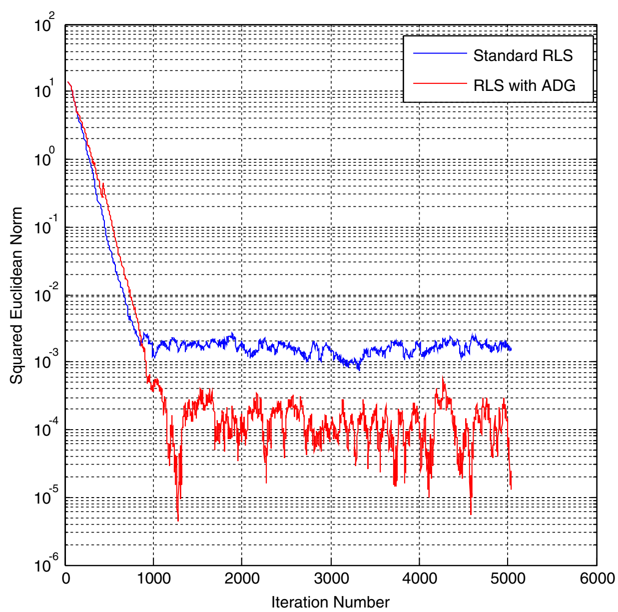

Fig. 14. Asymptotic behavior for the standard RLS algorithm and the RLS algorithm with ADG for white input.

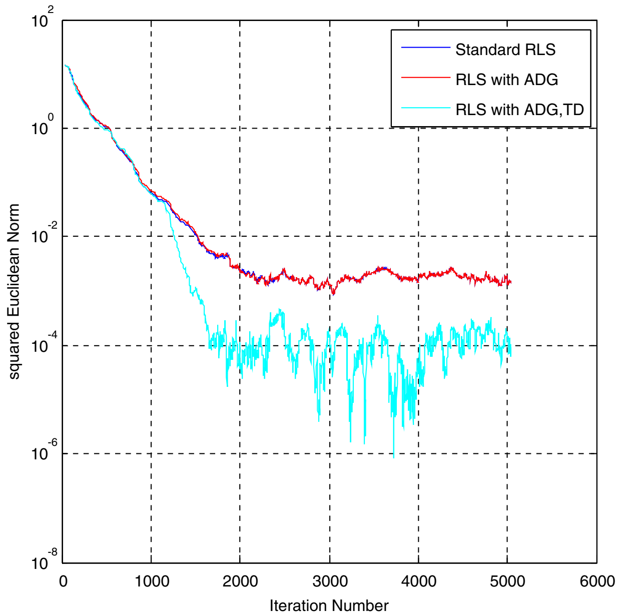

Fig. 15. Asymptotic behavior for the standard RLS algorithm, the RLS algorithm with ADG, and the RLS algorithm with ADG and TD for colored input.

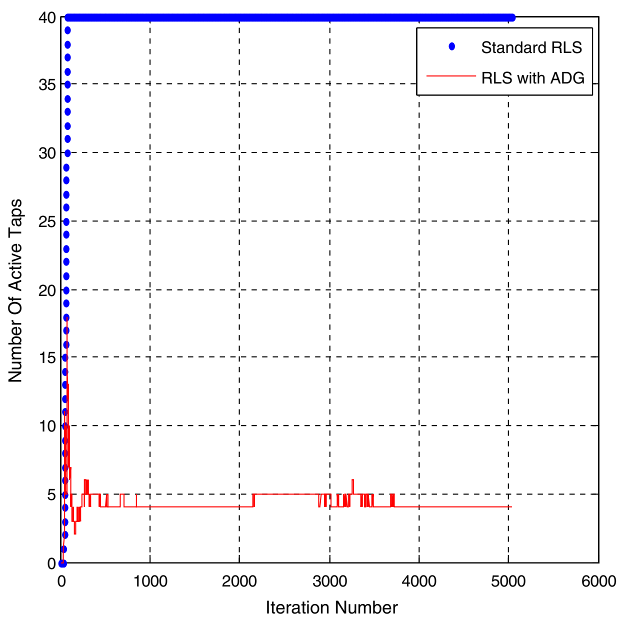

Fig. 16. Estimation of the number of active taps by the standard RLS algorithm and the RLS algorithm with ADG for white input.

D. Comparison Between LMS and RLS Adaptive Algorithms

It is known that the RLS algorithm has more computational complexity than that of the LMS algorithm. Figure 18 shows the estimated channel impulse response using the standard RLS algorithm. As shown, the standard RLS algorithm cannot solve the problem of ISI and cannot eliminate the inactive taps. On the other hand, Fig. 19 shows the estimated channel impulse response using the RLS algorithm with ADG and TD in the case of colored input signals. From these results, it can be revealed

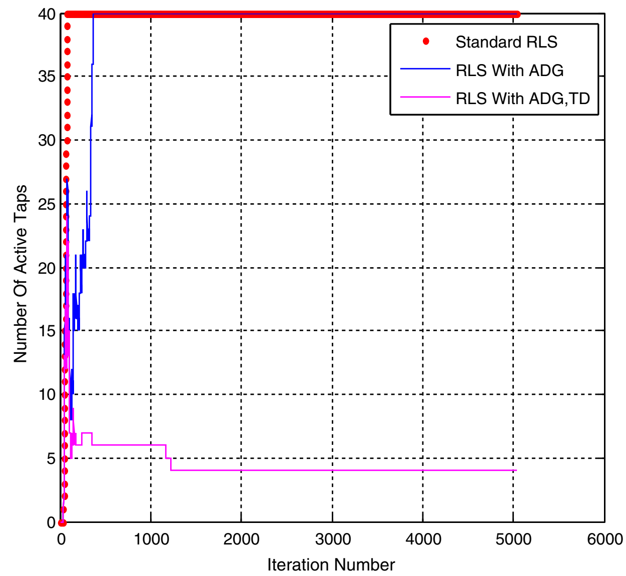

Fig. 17. Estimation of the number of active taps by the standard RLS algorithm, the RLS algorithm with ADG, and the RLS algorithm with ADG and TD for colored input.

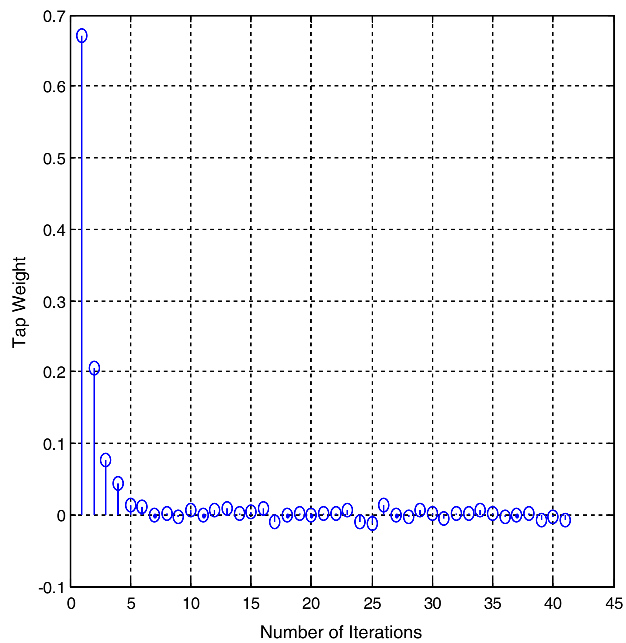

Fig. 18. Estimated channel impulse response using the standard RLS algorithm.

that the RLS algorithm with ADG and TD can distinguish between active and inactive taps, and hence it can be used effectively to combat the problem of ISI. Figures 20 and 21 compare the behavior of the RLS algorithm with ADG and TD with that of the LMS algorithm with ADG and TD from the perspectives of the squared weight-error performance and the number of estimated channel taps. From these two comparisons, it is clear that the RLS algorithm with ADG and TD has a faster convergence than the LMS algorithm with ADG and TD.

As shown in the simulation results, the proposed RLS algorithm with ADG and TD has been presented and tested to solve

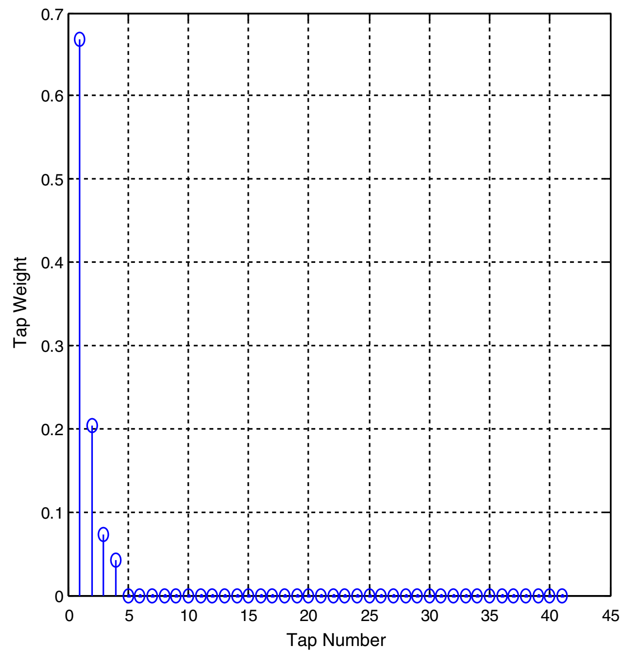

Fig. 19. Estimated channel impulse response using the RLS algorithm with ADG and TD.

the problem of ISI in diffuse indoor optical channels and has been compared to the standard adaptive LMS algorithm. The ADG and TD techniques have been used to distinguish between active and inactive estimated taps and prevent the coupling between them, and hence they mitigate the ISI problem. The RLS algorithm with ADG and TD has also been used to prevent ISI, and it shows a good performance in preventing ISI and estimating the channel impulse response without any tap coupling. Furthermore, the RLS algorithm with ADG and TD shows a faster convergence than that of the LMS algorithm with ADG and TD. So, it can be used effectively in nonstationary wireless optical channels.

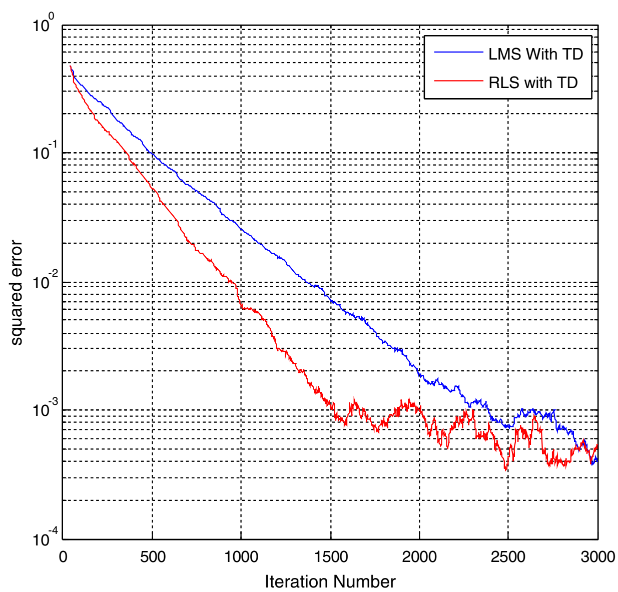

Fig. 20. Squared weight-error performance of the LMS algorithm with ADG and TD and the RLS algorithm with ADG and TD.

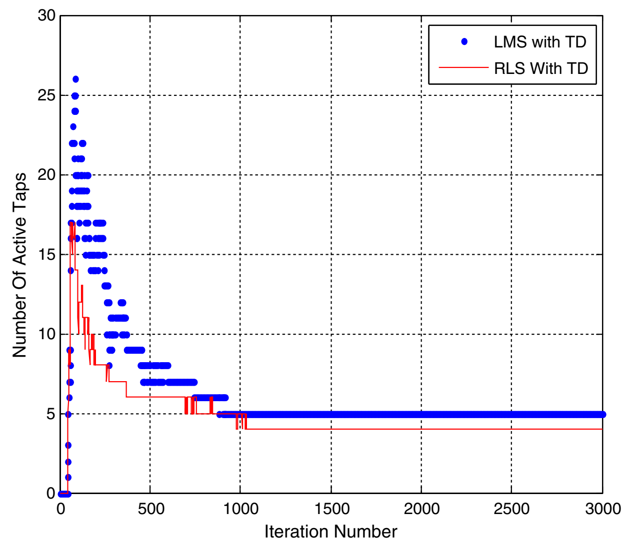

Fig. 21. Estimated channel taps using the LMS algorithm with ADG and TD and the RLS algorithm with ADG and TD.

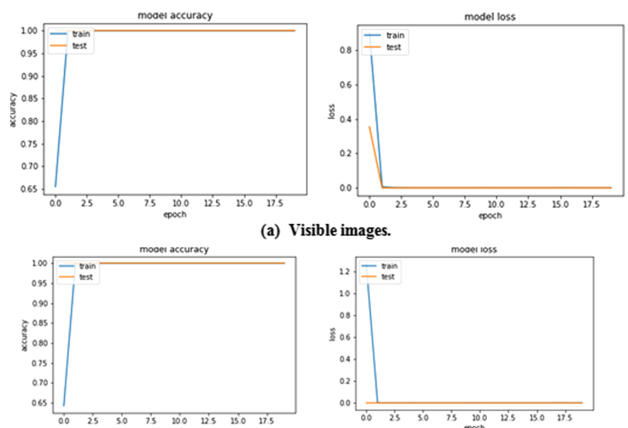

(a) Visible images.
(b) IR images.

Fig. 22. Accuracy and loss for training and testing phases along the epochs for (a) visible and (b) IR images.

E. Results of Image Quality Assessment

Simulation experiments have been carried out using Python 3.5 [34], TensorFlow [35], and Keras to test the performance of the proposed quality assessment algorithm of optical communication based on a CNN with the simulation parameters introduced in [32,33].

Figure 22 shows the accuracy and loss for training and testing phases along the epochs, for visible and IR images. Twenty epochs and a batch size of 10 have been adopted to train the model. From Fig. 22, it can be observed that the model achieves an accuracy of 100% for both IR and visible images.

6. CONCLUSION

In this research paper, an OWC framework for robust communication in African countries has been presented. The performance of this framework has been studied and investigated from different perspectives. Channel coding has been used to enhance the BER performance, and adaptive channel estimation has been investigated as an efficient tool for better channel equalization, and hence better performance enhancement. Moreover, a quality assessment algorithm based on CNNs for communication over optical links has been presented. Simulation results have proved that the BER performance of the ADO-OFDM system with LDPC coding is better than that with Hamming code, especially with low data rates at low DC biases. At high data rates, the error performance for coded ADO-OFDM with the Hamming coding gets close to its error performance with LDPC coding. In addition, with the increase of the DC bias, the Hamming code performance becomes better than that of the LDPC code. Generally, the increase of the DC bias means inefficient use of the system power, while a low DC value causes large clipping noise. Thus, we should have a balanced relation between system power consumption and clipping distortion. However, the LDPC code is recommended for higher code rates, as it has better coding performance and lower decoding complexity compared with those of the Turbo code. The simulation results revealed that the Hamming code has almost the same performance as that of the LDPC code at higher coding rates, with too small decoding time compared to the decoding time of the LDPC code. It is concluded from this research work that the Hamming code is recommended for low-to-moderate code rates because of its better BER performance. Moreover, the LMS and RLS adaptive channel estimation algorithms with ADG and TD have been investigated to mitigate the problem of ISI over OWC channels. They have been compared with the standard adaptive algorithms. The ADG and TD techniques have been used to distinguish between active and inactive estimated channel taps for preventing the coupling between taps, and hence mitigating the ISI problem. The proposed adaptive channel estimation algorithm shows fast convergence as well as good performance in estimating the channel impulse response. The simulation results revealed that the RLS algorithm with ADG and TD has a very good performance in OWC systems, as it can mitigate the problem of ISI. In addition, an efficient CNN-based algorithm has been presented in this paper for rating the communication quality over OWC channels. Simulation results on zebra chart patterns transmitted over the channels reveal a success rate of quality level classification of 100%. This research is very useful for developing countries in Africa, as it introduces an enhancement in the current and future applications of the OWC technology.

Disclosures. The authors declare no conflict of interest.

REFERENCES

1. M. Chowdhury, M. T. Hossan, A. Islam, and Y. M. Jang, "A comparative survey of optical wireless technologies: architectures and applications," IEEE Access **6**, 9819–9840 (2018).
2. M. N. O. Sadiku, S. M. Musa, and S. R. Nelatury, "Free space optical communications: an overview," Eur. Sci. J. **12**, 1857–7881 (2016).
3. Z. Ghassemlooy, W. Popoola, and S. Rajbhandari, *Optical Wireless Communications: System and Channel Modeling with MATLAB(R)*, 1st ed. (CRC Press, 2012).
4. A. K. Majumdar, *Modulation, Detection, and Coding for Free-space Optical (FSO) Communications*, Part of the Springer Series in Optical Sciences B series (SSOS) (2014), Vol. **186**, pp. 69–103.
5. J. Tan, K. Yang, and M. Xia, "Adaptive equalization for high speed optical MIMO wireless communications using white LED," Front. Optoelectron. **4**, 454–461 (2011).
6. Z. Ghassemlooy, H. L. Minh, S. Rajbhandari, J. Perez, and M. Ijaz, "Performance analysis of ethernet/fast-ethernet free space optical communications in a controlled weak turbulenc condition," J. Lightwave Technol. **30**, 2188–2194 (2012).
7. K. Ebihara, K. Kamakura, and T. Yamazato, "Spatially-modulated spacetime coding in visible light communications using 22 LED array," in *IEEE Asia Pacific Conference on Circuits and Systems (APCCAS)*, Ishigaki, Japan, 2014, pp. 320–323.
8. D. Zheng, Y. Li, H. Zhou, Y. Bian, C. Yang, W. Li, J. Qiu, H. Guo, X. Hong, Y. Zuo, I. P. Giles, W. Tong, and J. Wu, "Performance enhancement of free-space optical communications under atmospheric turbulence using modes diversity coherent receipt," Opt. Express **26**, 28879–28890 (2018).
9. M. A. Ali, "Atmospheric turbulence effect on free space optical communications," Int. J. Emerg. Technol. Comput. Appl. Sci. **5**, 345–351 (2013).
10. H. Kaushal and G. Kaddoum, "Optical communication in space: challenges and mitigation techniques," IEEE Commun. Surveys Tuts. **19**, 57–96 (2017).
11. G. A. Hussien, A. E. A. Mohamed, O. A. Oraby, E. S. Hassan, I. M. Eldokany, E.-S. M. El-Rabaie, M. I. Dessouky, S. A. Alshebeili, and F. E. Abd El-Samie, "Light wave transmission through free space using atmospheric laser links with adaptive equalization," Opt. Eng. **52**, 77–102 (2013).
12. S. M. Kuo, B. H. Lee, and W. Tian, *Real-Time Digital Signal Processing: Fundamentals, Implementations and Applications* (Wiley, 2013).
13. O. Ergul, E. Dinc, and O. B. Akan, "Communicate to illuminate: state-of-the-art and researchchallenges for visible light communications," Phys. Commun. **17**, 72–85 (2015).
14. J. Dang, Z. Zhang, and L. Wu, "A novel receiver for ACO-OFDM in visible light communication," IEEE Commun. Lett. **17**, 2320–2323 (2013).
15. N. Wu and Y. Bar-Ness, "A novel power-efficient scheme for asymmetrically and symetrically clipping optical (ASCOC)-OFDM for IM/DD optical systems," EURASIP J. Adv. Sig. Proc. **2015**, 3 (2015).
16. K. DeerghaRao, "Low density parity check codes," in *Channel Coding Techniques for Wireless Communications* (2015), pp. 251–303.
17. M. K. Abd-Ellah, A. I. Awad, A. A. M. Khalaf, and H. F. A. Hamed, "A review on brain tumor diagnosis from MRI Images: practical implications, key achievements, and lessons learned," Magn. Reson. Imaging **61**, 300–318 (2019).
18. S. N. Mohamed, A. N. A. Mohamed, F. E. Abd El-Samie, and A. N. Z. Rashed, "Performance enhancement of IM/DD optical wireless systems," Photon. Netw. Commun. **36**, 114–127 (2018).
19. S. D. Dissanayake and J. Armstrong, "Comparison of ACO-OFDM, DCO-OFDM and ADO-OFDM in IM/DD systems," J. Lightwave Technol. **31**, 1063–1072 (2013).
20. W. Xu, M. Wu, X. You, and C. Zhao, "ACO-OFDM-specified recoverable upper clipping with efficient detection for optical wireless communications," IEEE Photon. J. **6**, 7902617 (2014).
21. R. Bai, J. Chen, T. Mao, and Z. Wang, "Enhanced asymmetrically clipped DC biased optical OFDM for intensity-modulated direct-detection systems," J. Commun. Inf. Netw. **2**, 36–46 (2017).
22. M. Jiang, J. Zhang, X. Liang, and C. Zhao, "Direct current bias optimization of the LDPC coded DCO-OFDM systems," IEEE Photon. Technol. Lett. **27**, 2095–2098 (2015).
23. A. Tiwari and V. K. Sahu, "Error correction channel coding practices for wireless communication systems," Int. J. Adv. Res. Comput. Commun. Eng. **4**, 151–159 (2015).
24. A. Goel and M. Kumar Garg, "Comparative performance evaluation of convolutionally coded and LDPC coded OFDM system over AWGN and SUI-5 fading channel," in *3rd International Conference on Computer and Communication TechNology*, October 2012, pp. 250–254.
25. A. S. Hassan, M. Dessouky, A. Abou Elazm, and M. Shokair, "Evaluation of complexity versus performance for turbo code and LDPC under different code rates," in *SPACOMM 2012: The*

4th International Conference on Advances in Satellite and Space Communications (2012).

26. A. HadiSaleh, "Design of Hamming code for 64 bit single error detection and correction using VHDL," Diyala J. Eng. Sci. **8**, 22–37 (2015).
27. P. Di Lorenzo, S. Barbarossa, P. Banelli, and S. Sardellitti, "Adaptive least mean squares estimation of graph signals," IEEE Trans. Signal Inf. Process. Netw. **2**, 555–568 (2016).
28. I. E. Lee, Z. Ghassemlooy, W. P. Ng, and M. Uysal, "Performance analysis of free space optical links over turbulence and misalignment induced fading channels," in *8th International Symposium on Communication Systems, Networks & Digital Signal Processing (CSNDSP)*, July 18–20, 2012, pp. 1–6.
29. L. Mahmood, S. Shirazi, S. Naz, S. Shirazi, M. Razzak, A. Umar, and S. Ashraf, "Adaptive filtering algorithms for channel equalization in wireless communication," Indian J. Sci. Technol. **8**, 57805 (2015).
30. Manoj, M. Kumar, and K. Rohilla, "Adaptive equalization of fractionally spaced equalizer based on activity detection and tap decoupling," Int. J. Eng. Innov. Technol. **3**, 209–212 (2014).
31. U. Deol and Y. Juneja, "Activity detection using adaptive decision feedback optical equalizers (DFE) in optical communication," Int. J. Eng. Sci. Paradigms Res. **6** (2013).
32. A. A. Sadik and G. K. Salih, "A study in the effect of step-size of LMS algorithm in sparse channel estimation," Al-Ma'mon Coll. J. **2012** 301–312 (2012).
33. N. Srivastava, G. Hinton, A. Krizhevsky, I. Sutskever, and R. Salakhutdinov, "Dropout: A simple way to prevent neural networks from overfitting," J. Mach. Learn. Res. **15**, 1929–1958 (2014).
34. https://www.python.org/downloads/release/python-350/.
35. https://www.tensorflow.org/.